

Dynamics Parameters Identification of Rigid-Body Manipulators through Natural Oscillations

Rodrigo S. Jamisola, Jr.[†], Elmer P. Dadios[‡], and Marcelo H. Ang, Jr.*

Abstract—This work will present an experimental procedure in identifying the moments of inertia, mass, and center of mass of a rigid-body manipulator through natural oscillations. Based on the response of the manipulator, the values of the dynamics parameters to be identified are adjusted in such a way that the desired natural oscillation is achieved. The experiments to be performed on a manipulator under torque control are composed of two sets: mass and center of mass identification, and moments of inertia identification. The first set of experiments will use an open-loop control, such that the natural oscillation is minimized. The second set of experiments will use a proportional control, such that the square of the natural oscillation is equal to the proportional gain. Thus each set of experiments has a well-defined objective function such that it can be treated as an optimization computation. The correct dynamics parameters are identified when the desired objective function is achieved. The proposed dynamics identification method is analyzed and a theorem is presented to support the claims presented in this work, together with simulation results.

Index Terms—moment of inertia, mass, center of mass, identification experiment, dynamics model, natural oscillation, torque control

I. INTRODUCTION

A full dynamics control of a robot manipulator can only be achieved with accurate information on the manipulator's dynamics parameters. A very good performance in full dynamics simultaneous force and motion control shown in [1] was achieved because the manipulator dynamics were properly modeled and identified. The accuracy of dynamics modeling lies heavily on accurate values of the manipulator's dynamics parameters, namely, the moments of inertia, mass, and center of mass. Although some robot manufacturers do provide information on mass and center of mass parameters [2], the moments of inertia are not provided. One possible hesitation in providing the inertia values by manufacturers is the fact that at best, they only provide inertia values based on the type of material used and CAD drawing of the physical system. However, values derived through this method can be inadequate because of other factors like gear ratio and motor inertia, which could offset the true values of the inertia parameters.

But even if all the dynamics parameters are provided by a manufacturer, from the point of view of full dynamics control,

it would be good to verify the accurateness of the given values especially when the given manipulator has achieved thousands of hours of operation. Thus, an experimental procedure to identify the mass, center of mass, and inertia values can be more appropriate.

This work will propose an experimental procedure in identifying mass, center of mass, and inertia parameters through natural oscillation. The experiment sets the manipulator to achieve a linear second-order system response and its oscillation is measured. A well-defined value of the desired natural oscillation transforms the identification experiment into an optimization computation. The period of oscillation is minimized in the mass and center of mass identification with the manipulator under open-loop torque control. While in the inertia identification, the square of the period of oscillation is equal to the proportional gain, with the manipulator under proportional torque control.

There are several studies in inertia parameter identification designed to accurately model and control a physical system. Among such studies include a moment of inertia identification for mechatronic systems with limited strokes [3] in utilizing periodic position reference input identification of inertia based on the time average of the product of torque reference input and motor position. This study showed the moment of inertia error is within $\pm 25\%$. On tracking a desired trajectory and noting the error response, inertia parameters are identified using adaptive feedback control [4] where angular velocity tracking are observed and inertia parameters are changed, while a globally convergent adaptive tracking of angular velocity is shown in [5]. In other studies, least squares error in the response is used in inertial and friction parameters identification for excavator arms [6]. It is also used to identify inertias of loaded and unloaded rigid bodies for test facilities [7], and in another experimental set up [8].

Inertias that are dependent on the same joint variables, and is also referred to as the minimal linear combinations of the inertia parameters [9], can be combined to form lumped inertias. This inertia model has been shown even in an earlier work on a complete mathematical model of a manipulator [10]. In most cases lumped inertias, instead of individual inertias, are identified. This is because lumped inertias are easier to identify.

A similar work that identified lumped inertias through natural oscillation is shown in [11]. The shown full dynamics identification method was the foundation in a successful implementation of a mobile manipulator [1] performing an aircraft canopy polishing at a controlled normal force of 10 N. The biggest challenge in implementing the dynamics identification

[†]Dept. of Electronics and Communications Engineering and
[‡]Dept. of Manufacturing Engineering and Management, De La Salle University - Manila, 2401 Taft Ave, 1004 Manila, Philippines
{rodrigo.jamisola, elmer.dadios}@dlsu.edu.ph.

*Dept. of Mechanical Engineering, National University of Singapore, 21 Lower Kent Ridge Road, Singapore 119077 mpeangh@nus.edu.sg.

This work is supported by the University Research Council of De La Salle University - Manila.

in [11] is its need for a simplified symbolic model in order to identify the lumped inertias. Deriving the simplified symbolic model can become very computationally expensive when the number of degrees of freedom of the manipulator increases. In addition, the mass and center of mass were not identified and were assumed as given.

This work differs from [11] in the sense that the identification procedure proposed in this work does not require the simplified symbolic model because the individual inertias are identified, and not the lumped inertias. The mass and center of mass are individually identified as well. These two points comprise the major contributions of this work.

More recent identification procedures of manipulator arm dynamics include the use of torque data [12], floating-base motion dynamics [13], iterative learning [14], neural network aided identification [15], set membership uncertainty [16], and simultaneous identification and control [17]. Identification procedures that are more robot specific include [18], [19], [20], [21]. Some examples of identification procedures for humanoid robot dynamics used neural network [22], and fuzzy-stochastic functor machine [23]. Recent humanoid robot modeling and control include fuzzy neural network [24], global dynamics [25], and ground interaction control [26].

In most identification procedures the identification experiment is dependent on minimizing the least squares error based the robot response to a predefined path which excites the dynamics parameters. The controller used in the experimental procedures is the same controller that were used in the actual robot control. This approach can be at a disadvantage because characterizing a path that isolates the dynamics contribution of each parameter can be hard to find. Thus in some cases, the accurateness of each individual physical parameter values are at times compromised.

The experimental procedure proposed in this work make use of an independent controller and is dependent on each link achieving natural oscillation. The estimated values of the excited physical parameter can be verified by noting the change in the period of oscillation based on its predetermined value. The parameter estimates are adjusted such that the desired period of natural oscillation of a given link is achieved. This isolates each individual physical parameter estimate to the system response.

This work will propose an experimental procedure, based on natural oscillation, to identify the individual moment of inertia, mass, and center of mass parameters of rigid-body manipulators. The objective is to make the rigid-body manipulator achieve linear second-order response such that a desired value of its natural oscillation is known. When the desired natural oscillation is reached, the correct parameters are found. This work is aimed at providing an alternative in dynamics identification methods that is easily implementable, that identifies individual dynamics parameters, and with comparably accurate results. A theorem is presented to support the mathematical principles behind the experimental procedure together with experimental results.

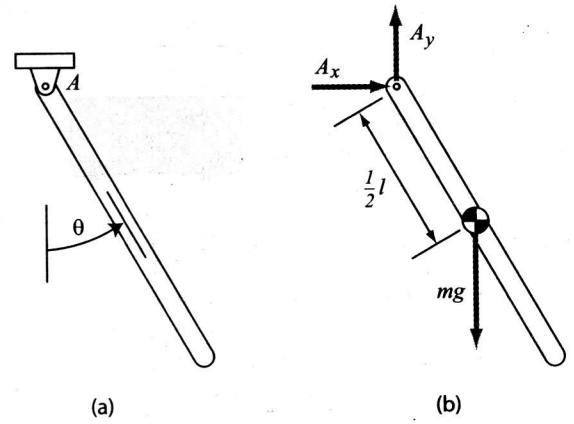


Fig. 1. Subfigure (a) shows an upright pendulum turning about point A due to gravity and an initial displacement from equilibrium position. Subfigure (b) shows the free body diagram.

II. OVERVIEW

A. Linear Second-Order Systems

The sum of the kinetic energy K and potential energy P of an upright pendulum, as shown in Fig. 1, consisting of a slender bar with mass m and length l is [27]

$$K + P = \frac{1}{2}I \left(\frac{d\theta}{dt} \right)^2 - \frac{1}{2}mgl \cos \theta \quad (1)$$

and is constant, where I is the inertia of the slender bar, g is the gravitational constant, and θ is the angular displacement from the vertical axis. Taking the time derivative and assuming small angular displacements, the above equation can be expressed as

$$\frac{d^2\theta}{dt^2} + \frac{mgl}{2I}\theta = 0 \quad (2)$$

with constant frequency of oscillation $\omega^2 = mgl/2I$. The system in (2) is a linear second-order system similar to a mass-spring oscillator shown in Fig. 2 which is defined by

$$\frac{d^2x}{dt^2} + \frac{k}{m}x = 0 \quad (3)$$

where the frequency of oscillation $\omega^2 = k/m$. The relationship in (2) shows the frequency of oscillation being dependent on the physical characteristic of the pendulum. Thus a different pendulum with different physical characteristics will give a different value of the frequency of oscillation. When no torque given at point A, the only moment acting on the pendulum is that due to gravity. When an initial displacement is given, it will cause the system to respond with angular acceleration and achieve natural oscillation.

Next we consider an inverted pendulum as shown in Fig. 3. This time, a torque τ_A is given at point A as shown in the free-body diagram of Subfigure (b). With the torque sent to the system that is equal to the moment due to gravity, the inverted pendulum will now “float” against gravity. When an initial push is given, the inverted pendulum will achieve angular acceleration such that the effective torque sent to the system is

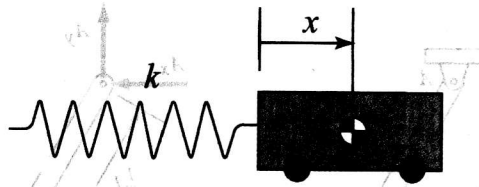


Fig. 2. A linear second-order system: spring-mass oscillator.

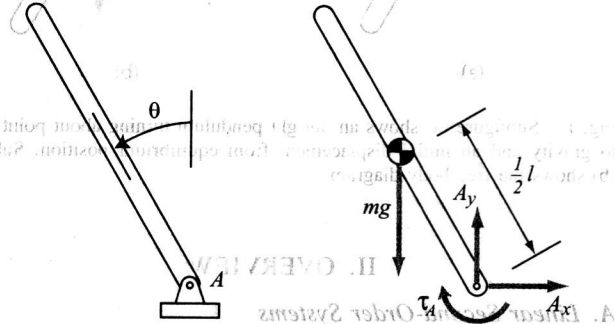


Fig. 3. Subfigure (a) shows an inverted pendulum. Subfigure (b) shows the free body diagram such that the gravitational compensation is sent to the system all the time which results into a system that is floating against gravity.

$$\tau_A = I\ddot{\theta} + \frac{1}{2}mgl\sin\theta \quad (4)$$

that is, the effective torque sent at point A is the sum of the given initial push that resulted into an acceleration and the torque sent to balance off gravity. An oscillation occurs because the total energy is in the process of being converted from a purely potential energy to a purely kinetic energy, and vice versa.

B. Mass and Center of Mass Identification

A torque control in (4) will equate the torque sent to the physical system to the torque sent to control it such that,

$$\tau_A = I\ddot{\theta} + \frac{1}{2}mgl\sin\theta = \tilde{I}u + \frac{1}{2}\tilde{m}g\tilde{l}\sin\theta \quad (5)$$

where \tilde{I} denotes the approximation of the actual physical system. Setting an open-loop control, $u = 0$, and assuming small angular displacements that is around ± 15 degrees, (5) becomes

$$\ddot{\theta} + \frac{ml - \tilde{m}\tilde{l}}{2I}g\theta = 0 \quad (6)$$

which is a linear second-order system where $\omega^2 = (ml - \tilde{m}\tilde{l})g/2I$. The minimum ω corresponds to $ml = \tilde{m}\tilde{l}$.

C. Moment of Inertia Identification

A proportional gain is set to (5) such that the control equation is expressed as $u = -k_p\theta$ where k_p is the proportional gain. Assuming that the gravitational term was correctly modeled, (5) can be expressed as a linear second-order system

$$\ddot{\theta} + \frac{\tilde{I}}{I}k_p\theta = 0 \quad (7)$$

where $\frac{\tilde{I}}{I}k_p = \omega^2$. Therefore, the inertia is correctly modeled when the frequency of oscillation $\omega^2 = k_p$.

D. Multi-Link Rigid-Body Dynamics

The general case of the multi-linked rigid body dynamics of a manipulator will be presented. The torque to be sent to each joint of the robot is computed by taking the kinetic energy K and potential energy P and solving the Lagrange equation of $T = K + P$ [28]

$$\frac{d}{dt} \left[\frac{\partial T}{\partial \dot{q}_i} \right] - \frac{\partial T}{\partial q_i} = \tau_i \quad (8)$$

such the joint torque vector is expressed as

$$\tau = \mathbf{A}(\mathbf{q})\ddot{\mathbf{q}} + \mathbf{c}(\mathbf{q}, \dot{\mathbf{q}}) + \mathbf{g}(\mathbf{q}) \quad (9)$$

The symbol $\mathbf{A}(\mathbf{q})$ is the joint-space inertia matrix, $\mathbf{c}(\mathbf{q}, \dot{\mathbf{q}})$ is the Coriolis and centrifugal forces vector, $\mathbf{g}(\mathbf{q})$ is the gravitational terms vector, and $\ddot{\mathbf{q}}, \dot{\mathbf{q}}, \mathbf{q}$ are the joint space acceleration, velocity, and displacement. The control equation is given as [29]

$$\mathbf{u} = \ddot{\mathbf{q}}_d + \mathbf{k}_v(\dot{\mathbf{q}} - \dot{\mathbf{q}}_d) + \mathbf{k}_p(\mathbf{q} - \mathbf{q}_d) \quad (10)$$

where \mathbf{k}_p is the proportional gain, \mathbf{k}_v is the derivative gain, and the subscript d denotes desired values. In addition to assuming small displacements during identification procedure, velocity for each link is assumed small such that Coriolis and centrifugal forces are less dominant compared to the gravitational forces, and the inertia matrix. These assumptions would lead to a linear-second order system that is equivalent to the single degree-of-freedom (DOF) case.

In [11], it is shown that the lumped inertia terms found in the inertia matrix $\mathbf{A}(\mathbf{q})$ are the same terms found in Coriolis and centrifugal forces vector $\mathbf{c}(\mathbf{q}, \dot{\mathbf{q}})$. Once all the lumped inertia terms are identified in $\mathbf{A}(\mathbf{q})$, all the inertia terms are already found.

III. THE PROPOSED DYNAMICS IDENTIFICATION METHOD

In this section we will show a mathematical proof of the proposed method to support the claims in this work in identifying mass, center of mass, and moment of inertia. In addition, corresponding algorithms will be shown.

A. Mass and Center of Mass Identification

Given a physical system such that each link is influenced by gravitational force, mass and center of mass can be identified by letting the system achieve natural oscillation through the force of gravity. It is assumed that the links move at small angular displacements around ± 15 degrees away from zero gravity axis. Friction contribution is disregarded in this work and will be addressed in the future.

Theorem 1: A multi-link rigid manipulator with revolute joints is under torque control and is influenced by gravitational force. Its minimum frequency of oscillation ω is achieved when the estimated physical parameter values in the mathematical model are closest to the values in the physical system.

Proof: Case I. Single Degree-of-Freedom. Equating the torque between the physical system and the mathematical model results in

$$\tau = I\ddot{\theta} + g(\theta) = \tilde{I}u + \tilde{g}(\theta), \quad (11)$$

where the control equation $u = \ddot{\theta}_d - k_v(\dot{\theta} - \dot{\theta}_d) - k_p(\theta - \theta_d)$. Setting $u = 0$ results into open-loop control such that

$$\ddot{\theta} + \frac{g(\theta) - \tilde{g}(\theta)}{I} = 0. \quad (12)$$

Because of relatively small angular displacements, (12) can be considered as an undamped linear second-order system [30] where

$$\omega^2 = f(g(\theta) - \tilde{g}(\theta)). \quad (13)$$

Because I is constant, ω is minimum when $g(\theta) = \tilde{g}(\theta)$.

Case II. Multiple Degree-of-Freedom. The torques sent to the physical system and the mathematical model are equal and can be expressed as,

$$\tau = \mathbf{A}(\theta)\ddot{\theta} + \mathbf{c}(\theta, \dot{\theta}) + \mathbf{g}(\theta) = \tilde{\mathbf{A}}(\theta)\mathbf{u} + \tilde{\mathbf{c}}(\theta, \dot{\theta}) + \tilde{\mathbf{g}}(\theta). \quad (14)$$

With relatively small joint velocities, Coriolis and centrifugal forces are less dominant and are ignored. With small angular displacements, gravitational terms can be considered linear. Setting the control equation $\mathbf{u} = \mathbf{0}$ results into

$$\ddot{\theta} + \mathbf{A}(\theta)^{-1}[(\mathbf{g}(\theta) - \tilde{\mathbf{g}}(\theta))]. \quad (15)$$

With the small angular displacement $\mathbf{A}(\theta)$ can be considered constant. As the correct parameter values are approached, the system becomes decoupled such that each link can be independently considered as second-order undamped linear system [30] where

$$\omega^2 = f(\mathbf{g}(\theta) - \tilde{\mathbf{g}}(\theta)). \quad (16)$$

The minimum ω is achieved when $\mathbf{g}(\theta) = \tilde{\mathbf{g}}(\theta)$. ■

B. Moment of Inertia Identification

Given a physical system with its gravitational model correctly compensated (or is independent of the gravitational effect), the inertia parameters can be identified by letting the system achieve its natural frequency of oscillation. The inertia values will be adjusted until the desired frequency response is achieved. The following corollary follows the theorem presented above.

Corollary 1: A rigid manipulator under proportional torque control is not influenced by gravity. The correct values of link inertia parameters are identified when $\omega^2 = k_p$ where ω is

the natural frequency of oscillation and k_p is the proportional gain.

Proof: Case I. Single Degree-of-Freedom. Equating the torque between the physical system and the mathematical model,

$$\tau = I\ddot{\theta} + g(\theta) = \tilde{I}u + \tilde{g}(\theta), \quad (17)$$

The proportional control is set to $u = -k_p\theta$ and the rest of the control terms are set to zero, $k_v = 0$ and $\ddot{\theta}_d = \dot{\theta}_d = \theta_d = 0$. Because the gravity has no influence or is correctly modeled, the equation becomes

$$\ddot{\theta} + \frac{\tilde{I}}{I}k_p\theta = 0. \quad (18)$$

This is an undamped linear second-order system [30] such that,

$$\omega^2 = \frac{\tilde{I}}{I}k_p. \quad (19)$$

When $\tilde{I} = I$, then $k_p = \omega^2$.

Case II. Multiple Degree-of-Freedom. The torques sent to both the physical system and the mathematical model are equal and expressed as,

$$\tau = \mathbf{A}(\theta)\ddot{\theta} + \mathbf{c}(\theta, \dot{\theta}) + \mathbf{g}(\theta) = \tilde{\mathbf{A}}(\theta)\mathbf{u} + \tilde{\mathbf{c}}(\theta, \dot{\theta}) + \tilde{\mathbf{g}}(\theta). \quad (20)$$

Setting the proportional control to $\mathbf{u} = -\mathbf{k}_p\theta$ and the rest of the control terms are set to zero, $\mathbf{k}_v = \mathbf{0}$ and $\ddot{\theta}_d = \dot{\theta}_d = \theta_d = \mathbf{0}$. With slow velocities the Coriolis and centrifugal terms are less dominant and can be ignored. And because gravity has no influence or is correctly modeled,

$$\ddot{\theta} + \mathbf{A}(\theta)^{-1}\tilde{\mathbf{A}}(\theta)\mathbf{k}_p\theta = 0. \quad (21)$$

As the system approaches the correct parameter values, it becomes decoupled such that each link can be independently considered as second-order undamped linear system [30] where

$$\omega^2 = \mathbf{A}(\theta)^{-1}\tilde{\mathbf{A}}(\theta)\mathbf{k}_p. \quad (22)$$

The case of $\tilde{\mathbf{A}}(\theta) = \mathbf{A}(\theta)$ results in $\omega^2 = \mathbf{k}_p$. ■

C. The Algorithm

The algorithm for identifying mass, center of mass, and moment of inertia through natural oscillation is presented in this subsection. For mass and center of mass, the identification procedure is the following.

- 1) Select initially large values for the mass \tilde{m} , and center of mass \tilde{r} to initialize the dynamics parameters of the multi-link rigid body.
- 2) For each of the joint, send the torque τ corresponding to the Coriolis and centrifugal forces and the gravitational terms.
- 3) Let each link oscillate from a predefined initial displacement, to help create consistency of results. The system will start to oscillate at a certain frequency ω .
- 4) Measure the frequency of oscillation ω .

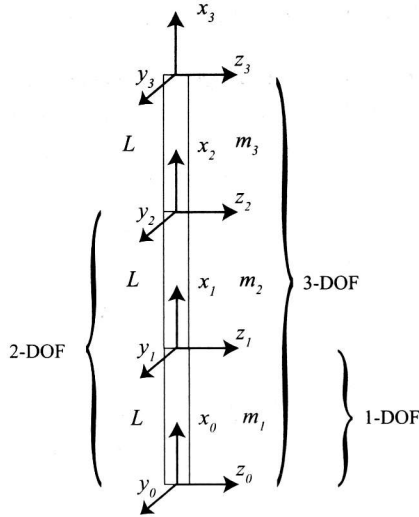


Fig. 4. The frame assignment for 1-DOF, 2-DOF, and 3-DOF manipulators.

- 5) Adjust the values of the dynamics parameters \tilde{m} , and \tilde{r} to minimize the frequency of oscillation ω .
- 6) Repeat Steps 2-5 until the minimum frequency of oscillation ω is found such that its corresponding \tilde{m} , and \tilde{r} are the best estimates.

In identifying moments of inertia \tilde{I} , the same algorithm as stated above will be used, except that \tilde{I} is the unknown parameter instead of \tilde{m} and \tilde{r} . Then instead of minimizing ω , the corresponding objective value of the frequency of oscillation will be $\omega^2 = k_p$.

The large values of the initial dynamics parameters are recommended to have an initially large solution space to explore. A predefined initial displacement is used to create consistent results in measuring the frequency of oscillation. The predefined value of this initial displacement should be about ± 15 degrees and with alternating opposite signs on consecutive joints. This setup will help minimize the displacement for each joint such that the assumption on linearity of the manipulator response will hold. In addition, this will also minimize the contribution of Coriolis and centrifugal forces such that the accumulated displacement of each joint remains small.

To measure the frequency of oscillation ω , normally the number of periods of oscillation is counted within a predefined number of update cycles. An incremental step is performed within the search space of the dynamics parameters to find the combination of values that correspond to the desired ω . The dimension of the search space increases as the number of dynamics parameters to be identified increases. Incrementally changing the values of the dynamic parameters and measuring the corresponding frequency of oscillation are repeatedly performed. For higher degrees of freedom, it is highly possible that the identified parameters will result in a combination of possible range of values. Each of the possible combinations can be checked later against the robot response in the actual manipulator control.

IV. RESULTS AND ANALYSIS

Simulations are performed to test the proposed algorithm in identifying the dynamics parameters of 1-, 2-, and 3-DOFs manipulators. Open dynamics engine (ODE), an OpenGL program integrated with C code, is used as the simulation platform. This simulation platform requires the actual physical model for the system to move in a virtual world. The dynamics parameters are then provided to create a model for the simulation. Then the corresponding torques are sent to the joints using estimated dynamics parameter values.

In this section, the range of estimated values corresponding to the desired ω will be presented for each of the simulated manipulator. The frame assignment is shown in Fig 4. The simplified symbolic dynamics model of 1-,2-, and 3-DOFs manipulators shown here are expressed in terms of masses and center, including the inertias. Corresponding mass factors are used to vary the possible range of values for the mass, center of mass, and inertia parameters. The following symbol simplifications are used $S_{i\dots n} = \sin(\sum_i^n \theta_i)$ and $C_{i\dots n} = \cos(\sum_i^n \theta_i)$.

A. One Degree of Freedom

The simplest case of 1-DOF is shown to test the sensitivity of the system to numerical errors. Given a mass m_1 and link length L , a mass factor fm_1 and fm_2 are multiplied to the gravitational and inertial terms, respectively.

$$\begin{aligned} I_1 &= fm_2 \frac{1}{3} m_1 L^2 \\ g_1 &= fm_1 \frac{1}{2} m_1 g L S_1. \end{aligned} \quad (23)$$

An initial 15 degrees displacement was used to perturb the system and let it achieve natural oscillation. The results are shown in Table I for the mass and center of mass and Table II for the moment of inertia.

TABLE I
MASS AND CENTER OF MASS IDENTIFICATION FOR 1-DOF

Mass Factor fm_1	No. of Periods at 5,000 Updates
1.020	8.7
1.010	6.9
1.005	5.8
1.004	5.5
1.003	5.1
1.002	4.8
1.001	4.2
1.000	4.1
0.999	(falls under gravity)

The correct values of the dynamics parameters correspond to $fm_1 = fm_2 = 1.00$. Table I shows consistently that as the estimated parameters start from large values and decrease towards the correct values, the frequency of oscillation decreases. And at 0.001 difference of the mass factor, a difference in the frequency of oscillation is achieved. The minimum frequency of oscillation is shown to be 4.1 periods per 5,000 update cycles. A mass factor $fm_1 = 0.999$ will cause the system to fall due to gravitational force. Table II shows consistently that as the mass factor increases, that is, the inertia estimates become larger than the actual values, the frequency of oscillation increases. It can be safely assumed that the

TABLE II
INERTIA IDENTIFICATION FOR 1-DOF

Mass Factor fm_2	No. of Periods at 20,000 Updates Link 1
1.00	35.50
1.01	35.57
1.02	36.00
1.03	36.00
1.04	36.10
1.05	36.50
1.06	36.62
1.07	36.60
1.08	37.00
1.09	37.00
1.10	37.13

difference in the frequency of oscillation is more elaborate when the mass factor changes to around 5%. It is also possible to increase the number of sampling updates in order to make more elaborate differences in the frequency of oscillation. An analytical sensitivity analysis on the mass and center of mass identification error as compared to the inertia identification error will be shown after this section.

B. Two Degrees of Freedom

The symbolic form of the components of inertia $\mathbf{A}(\theta)$, Coriolis and centrifugal forces $\mathbf{c}(\theta, \dot{\theta})$ and gravitational terms $\mathbf{g}(\theta)$ of the 2-DOFs manipulator is shown in (24).

$$\begin{aligned}
 A_{11} &= fm_4 \frac{1}{3} m_1 L^2 + fm_3 m_2 L^2 \left(\frac{4}{3} + C_2 \right) \\
 A_{12} &= A_{21} = fm_3 m_2 L^2 \left(\frac{1}{3} + \frac{1}{2} C_2 \right) \\
 A_{22} &= fm_3 \frac{1}{3} m_2 L^2 \\
 c_1 &= -fm_3 \frac{1}{2} m_2 L^2 \dot{q}_2 (2\dot{q}_1 + \dot{q}_2) S_2 \\
 c_2 &= fm_3 \frac{1}{2} m_2 L^2 S_2 \dot{q}_1^2 \\
 g_1 &= fm_1 \left(\frac{1}{2} m_1 + m_2 \right) L g S_1 + fm_2 \frac{1}{2} m_2 L g S_{12} \\
 g_2 &= fm_2 \frac{1}{2} m_2 L g S_{12}
 \end{aligned} \tag{24}$$

In the symbolic model shown, the mathematical model of the inertias were simplified such that only the principal moment of inertia about the joint axis is considered. The other two principal moments of inertia and all the products of inertia were assumed zero. However, in the simulation model this is not true, as the ODE simulation mimics the real-world physical system these values can only be assigned relatively small values and not completely zeros.

For each of the lumped inertia parameters, mass factors fm_1 , fm_2 , fm_3 , and fm_4 are used. Note that the dynamics model can be identified individually without the lumped symbolic model. However, the value of the lumped model only served to show the limits on the products of the identified parameters. In a sense it is the lumped model that is identified such that any values of m_1 and L would suffice to model the dynamics parameters as long as the product of their values corresponding to the actual physical model and is correct to within a desired accuracy. This precision defines the range of possible identified values.

Table III shows the experimental results for 5,000 updates of a two degrees of freedom robot with varying mass factors

TABLE III
MASS AND CENTER OF MASS IDENTIFICATION FOR 2-DOFS

Mass Factor fm_1, fm_2	No. of Periods at 5,000 Updates Link 1, Link 2
1.010	5.4
1.005	4.7
1.004	4.5
1.003	4.5
1.002	4.4
1.001	4.2
1.000	4.0
0.999	3.6
0.998	(falls under gravity)

TABLE IV
INERTIA IDENTIFICATION FOR 2-DOFS

Mass Factor fm_3, fm_4	No. of Periods at 20,000 Updates Link 1, Link 2
1.00	35.50
1.01	35.61
1.02	36.00
1.03	36.00
1.04	36.14
1.05	36.50
1.06	36.50
1.07	36.66
1.08	37.00
1.09	37.00
1.10	37.17

fm_1 and fm_2 . The frequency of oscillation is recorded for the different values of the mass factors. The robot falls under the influence of gravity when the mass factors are 0.002 below the assigned physical mass factor of 1.0. The minimum frequency of oscillation applies when all mass factors are 0.001 below 1.0. The frequencies of oscillations for both links decreased accordingly as estimated values decreased towards the actual physical values.

Table IV shows the experimental results for 20,000 updates of a two degrees of freedom robot with two mass factors fm_3 and fm_4 being varied. The frequency of oscillation is recorded for the different values of the mass factors. A mass factor of 1.0 corresponds to the correct natural frequency $\omega^2 = k_p$. The frequencies of oscillations for both links increased accordingly as the mass factor were increased. Again around 5% difference in the mass factor created an elaborate difference in the recorded period of oscillation.

$$\begin{aligned}
A_{11} &= fm_7 \frac{1}{3} (m_1 + 4m_2 + 7m_3) L^2 + fm_5 (m_2 + 2m_3) L^2 C_2 \\
&\quad + fm_4 m_3 L^2 (C_3 + C_{23}) \\
A_{12} &= A_{21} = fm_6 \frac{1}{3} (m_2 + 4m_3) L^2 + fm_5 \frac{1}{2} (m_2 + 2m_3) L^2 C_2 \\
&\quad + fm_4 \frac{1}{2} m_3 L^2 (2C_3 + C_{23}) \\
A_{13} &= A_{31} = fm_4 \frac{1}{6} m_3 L^2 (2 + 3C_3 + 3C_{23}) \\
A_{23} &= A_{32} = fm_4 \frac{1}{6} m_3 L^2 (2 + 3C_3) \\
A_{22} &= fm_6 \frac{1}{3} (m_2 + 4m_3) L^2 + fm_4 3m_3 L^2 C_3 \\
A_{33} &= fm_4 \frac{1}{3} m_3 L^2 \\
c_1 &= -fm_5 \frac{1}{2} (m_2 + 2m_3) L^2 \dot{q}_2 (2\dot{q}_1 + \dot{q}_2) S_2 \\
&\quad - fm_4 \frac{1}{2} m_3 L^2 (\dot{q}_3 (2\dot{q}_1 + 2\dot{q}_2 + \dot{q}_3) S_3 \\
&\quad\quad + (\dot{q}_2 + \dot{q}_3) (2\dot{q}_1 + \dot{q}_2 + \dot{q}_3) S_{23}) \\
c_2 &= fm_5 \frac{1}{2} (m_2 + 2m_3) L^2 \dot{q}_1^2 S_2 \\
&\quad + fm_4 \frac{1}{2} m_3 L^2 (-\dot{q}_3 (2\dot{q}_1 + 2\dot{q}_2 + \dot{q}_3) S_3 \\
&\quad\quad + \dot{q}_1^2 S_{23}) \\
c_3 &= fm_4 \frac{1}{2} m_3 L^2 ((\dot{q}_1 + \dot{q}_2)^2 S_3 + \dot{q}_1^2 S_{23}) \\
g_1 &= fm_1 \frac{1}{2} (m_1 + 2(m_2 + m_3)) Lg S_1 \\
&\quad + fm_2 \frac{1}{2} (m_2 + 2m_3) Lg S_{12} \\
&\quad\quad + fm_3 \frac{1}{2} m_3 Lg S_{123} \\
g_2 &= fm_2 \frac{1}{2} (m_2 + 2m_3) Lg S_{12} \\
&\quad + fm_3 \frac{1}{2} m_3 Lg S_{123} \\
g_3 &= fm_3 \frac{1}{2} m_3 Lg S_{123}
\end{aligned}
\tag{25}$$

C. Three Degrees of Freedom

The symbolic full dynamics model of a 3-DOFs is shown in (25). The link masses are m_1 , m_2 , and m_3 for links 1 to 3 and have equal link lengths of L .

Mass factors fm_1 , fm_2 , and fm_3 are used for the mass and center of mass identification, while mass factors from fm_4 to fm_7 are used for the lumped inertia parameters identification. It is assumed that the principal inertias of each link about the joint is dominant, such that the other principal inertias and the products of inertia are assumed zero. The inertias are expressed as masses and centers of mass. The values of fm_1 to fm_3 are varied to determine the system response at minimum ω , while the values of fm_4 to fm_7 are varied to determine the system response in finding $\omega^2 = k_p$.

Tables V and VI show the experimental response of the 3-DOF manipulator. In the experiment, the natural oscillation is achieved at slow speed and the entire system moves in unison. This is helpful but not necessary, in achieving well-defined natural oscillations. The inertias were also expressed in terms of masses and centers of mass, and the dominant parameters are gravitational and not the Coriolis and centrifugal forces.

As in the previous results, there is a distinctive decrease of the period of oscillation as the mass factors fm_1 , fm_2 , and fm_3 decrease towards the correct value. At mass factors of 0.998 the system fell under gravity. The minimum frequency of oscillation is achieved at a mass factor value of 0.999. The system can be considered as having a tolerance limit of ± 0.001 . Such tolerance value is also demonstrated in mass

TABLE V
MASS AND CENTER OF MASS IDENTIFICATION FOR 3-DOFS

Mass Factor fm_1, fm_2, fm_3	No. of Periods at 5,000 Updates Link 1, Link 2, Link 3
1.010	4.5
1.005	4.0
1.004	3.9
1.003	3.9
1.002	3.7
1.001	3.2
1.000	3.1
0.999	3.0
0.998	(falls under gravity)

TABLE VI
INERTIA IDENTIFICATION FOR 3-DOFS

Mass Factor fm_4, fm_5, fm_6, fm_7	No. of Periods at 20,000 Updates Link 1, Link 2, Link 3
1.00	35.50
1.01	35.62
1.02	36.00
1.03	36.00
1.04	36.14
1.05	36.50
1.06	36.50
1.07	36.66
1.08	37.00
1.09	37.00
1.10	37.18

factor values of 1.004 and 1.003 where the corresponding periods remain the same. For practical purposes, it can be stated that the tolerance value is at ± 0.002 . In the inertia identification, there is a distinctive difference in the period of oscillation when the mass factors fm_4 , fm_5 , fm_6 , and fm_7 differ by around 5%. Again, increasing the sampling update cycles can make the difference in the frequency of oscillations more elaborate for the same mass factor range.

The initial values were purposely chosen to be not too far from the real values (at a maximum of 10%) to show the sensitivity of the system to numerical errors when the estimated values are getting closer to the physical values. This is important because this will show the degree of precision in the proposed method's estimation ability. Because the proposed method converts the identification procedure into an optimization computation, convergence from a given set of initial values will be dependent on the optimization procedure used. One optimization procedure that may be used is the probabilistic gradient descent method that will perform a predefined number of random walks upon convergence. In this way, the computation can increase the probability of getting out of local minima.

In most cases, it is hard to quantify the acceptable tolerance values of an identified parameter because, to the best of our knowledge, there is no such quantification study. The correctness of the identified value is only checked through the accuracy of the robot response. But even with the quantification of the accuracy of robot response, there is no set standard on how much is the tolerance limit to be considered "best performance" given set parameters as speed, task requirement, and load. Thus the success of most dynamics identification

method normally is based on response of the manipulator where the identification is being implemented. And this is dependent on what type of task the manipulator is required to perform, and is generally not applicable to all systems.

V. SENSITIVITY ANALYSIS

Identifying the inertia parameters, together with the mass and center of mass, can create different errors in the torque response due to inaccuracy in the identified parameters. This section will show sensitivity to parameter errors in terms of gravitational terms as compared to inertial terms, and how both terms affect the error in torques. For simplify, sensitivity analysis is performed for 1-DOF manipulator.

Given a computed torque control where the dynamics parameters are correctly modeled under proportional control is expressed as

$$\tau = -\tilde{I} k_p e_\theta + \tilde{g} \quad (26)$$

where $e_\theta = \theta_d - \theta$. Then, given a perturbation in the gravitational model, $\delta\tilde{g}$, the resulting perturbed computed torque will be

$$\tau + \delta\tau_g = -\tilde{I} k_p e_\theta + (\tilde{g} + \delta\tilde{g}) \quad (27)$$

such that, the torque perturbation divided by the computed torque is

$$\frac{\delta\tau_g}{\tau} = \frac{\delta\tilde{g}}{-\tilde{I} k_p e_\theta + \tilde{g}} \quad (28)$$

On the other hand, given a perturbation in the inertia model, $\delta\tilde{I}$, the resulting perturbed computed torque is,

$$\tau + \delta\tau_I = -(\tilde{I} + \delta\tilde{I}) k_p e_\theta + \tilde{g} \quad (29)$$

and

$$\frac{\delta\tau_I}{\tau} = \frac{-\delta\tilde{I} k_p e_\theta}{-\tilde{I} k_p e_\theta + \tilde{g}} \quad (30)$$

Clearly, (30) showed that an error in the inertia identification has less effect than an error in gravitational term identification as shown in (28). This is because (30) is dependent on the error term e_θ which can become very small as the gain compensates for the error. Compared to (28), the error in gravitational term can never be compensated.

VI. CONCLUSION AND FUTURE WORK

This work showed a new method in identifying the mass, center of mass, and inertia parameters of a rigid-body manipulator through natural oscillation ω . A mathematical proof is presented to support the validity of the proposed algorithm. The correct values of the dynamics parameters correspond to the minimum frequency of oscillation ω for the mass and center of mass identification, and $\omega^2 = k_p$ for the inertia identification. Results sensitivity and range of the identified experimental values were shown for one, two, and three degrees of freedom manipulators, as well as sensitivity analysis on errors of identified inertia and gravitational parameters. The

future direction of this work is to implement the method on a physical robot manipulator, where the friction parameters influence the results. The ultimate goal of this experimental procedure is to implement it on a humanoid robot moving in a full-dynamics whole-body control [31].

VII. ACKNOWLEDGEMENT

The authors would like to acknowledge the research support given by the University Research Council of De La Salle University - Manila.

REFERENCES

- [1] R. S. Jamisola, Jr., D. N. Oetomo, J. M. H. Ang, O. Khatib, T. M. Lim, and S. Y. Lim, "Compliant motion using a mobile manipulator: An operational space formulation approach to aircraft canopy polishing," *RSJ Advanced Robotics*, vol. 19, no. 5, pp. 613-634, 2005.
- [2] L. Mitsubishi Heavy Industries, *PA-10 Portable General Purpose Intelligent Arm Operating Manual*, Kobe Shipyard and Machinery Works, Kobe, Japan, 1999.
- [3] F. Andoh, "Moment of inertia identification using the time average of the product of torque reference input and motor position," *IEEE Transactions on Power Electronics*, vol. 22, no. 6, pp. 2534-2542, Nov. 2007.
- [4] N. A. Chaturvedi, A. K. Sanyal, M. Chellappa, J. L. Valk, N. H. McClamroch, and D. S. Bernstein, "Adaptive tracking of angular velocity for a planar rigid body with unknown models for inertia and input nonlinearity," *IEEE Transactions on Control Systems Technology*, vol. 14, no. 4, pp. 613-627, Jul. 2006.
- [5] N. A. Chaturvedi, D. S. Bernstein, J. Ahmed, F. Bacconi, and N. H. McClamroch, "Globally convergent adaptive tracking of angular velocity and inertia identification for a 3-dof rigid body," *IEEE Transactions on Control Systems Technology*, vol. 14, no. 5, pp. 841-853, Sept. 2006.
- [6] S. Tafazoli, P. D. Lawrence, and S. E. Salcudean, "Identification of inertial and friction parameters for excavator arms," *IEEE Transactions on Robotics and Automation*, vol. 15, no. 5, pp. 966-971, Oct. 1999.
- [7] H. Hahn, K.-D. Leimbach, and A. Piepenbrink, "Inertia parameter identification of rigid bodies using a multi-axis test facility," in *Proceedings of the 3rd IEEE Conference on Control Applications*, Glasgow, Scotland, Aug. 24-26 1994, pp. 1735-1737.
- [8] H. Hahn and M. Niebergall, "Development of a measurement robot for identifying all inertia parameters of a rigid body in a single experiment," *IEEE Transactions on Control Systems Technology*, vol. 9, no. 2, pp. 416-423, Mar. 2001.
- [9] S.-K. Lin, "Minimal linear combinations of the inertia parameters of a manipulator," *IEEE Transactions on Robotics and Automation*, vol. 11, no. 3, pp. 360-373, June 1995.
- [10] H. Olsen and G. Bekey, "Identification of parameters in models of robots with rotary joints," in *Proceedings IEEE International Conference on Robotics and Automation*, St. Louis, MO, March 25-28 1985, pp. 1045-1049.
- [11] R. S. Jamisola, Jr., M. Ang, Jr., T. M. Lim, O. Khatib, and S. Y. Lim, "Dynamics identification and control of an industrial robot," in *Proceedings 9th International Conference on Advanced Robotics*, Tokyo, Japan, Oct. 25-27 1999, pp. 323-328.
- [12] M. Gautier, A. Janot, and P. Vandanjon, "Didim: A new method for the dynamic identification of robots from only torque data," in *Proceedings of the 2008 IEEE International Conference on Robotics and Automation*, Pasadena, CA, USA, May 19-23 2008, pp. 2122-2127.
- [13] K. Ayusawa, G. Venture, and Y. Nakamura, "Identification of humanoid robots dynamics using floating-base motion dynamics," in *Proceedings of the 2008 IEEE/RSJ International Conference on Intelligent Robots and Systems*, Nice, France, Sept. 22-26 2008, pp. 2854-2859.
- [14] B. Bukkens, D. Kostić, B. de Jager, and M. Steinbuch, "Learning-base identification and iterative learning control of direct-drive robots," *IEEE Transactions on Control Systems Technology*, vol. 13, no. 4, pp. 537-549, Jul. 2005.
- [15] Z.-H. Jiang, T. Ishida, and M. Sunawada, "Neural network aided dynamic parameter identification of robot manipulators," in *Proceedings of the 2006 IEEE International Conference on Systems, Man, and Cybernetics*, Taipei, Taiwan, Oct. 8-11 2006, pp. 3298-3303.

- [16] N. Ramdani and P. Poignet, "Robust dynamic experimental identification of robots with set membership uncertainty," *IEEE/ASME Transactions on Mechatronics*, vol. 10, no. 2, pp. 253–256, Apr. 2005.
- [17] D. J. Austin, "Simultaneous identification and control of a hybrid dynamic model for a mobile robot," in *Proceedings of the 39th Conference on Decision and Control*, Sydney, Australia, Dec., year =, pp. 3138–3143.
- [18] K. Radkhah, D. Kulic, and E. Croft, "Dynamic parameter identification for the CRS A460 robot," in *Proceedings of the 2007 IEEE/RSJ International Conference on Intelligent Robots and Systems*, San Diego, CA, USA, Oct. 29–Nov. 2 2007, pp. 3842–3847.
- [19] J. Swevers, W. Verdonck, and J. D. Schutter, "Dynamic model identification for industrial robots," in *IEEE Control Systems Magazine*, vol. 27, no. 5, Oct. 2007, pp. 58–71.
- [20] D. Kostić, B. de Jager, M. Steinbuch, and R. Hensen, "Modeling and identification for high-performance robot control: An RRR-robotic arm case study," *IEEE Transactions on Control Systems Technology*, vol. 12, no. 6, pp. 904–919, Nov. 2004.
- [21] N. A. Bompos, P. K. Artemiadis, A. S. Oikonomopoulos, and K. J. Kyriakopoulos, "Modeling, full identification and control of the mitsubishi pa-10 robot arm," in *Proceedings of the 2007 IEEE/ASME International Conference on Advanced Intelligent Mechatronics (AIM2007)*, Zurich, Switzerland, Sept. 5–7 2007, pp. 1–6.
- [22] K. Noda, M. Ito, Y. Hoshino, and J. Tani, "Dynamic generation and switching of object handling behaviors by a humanoid robot using a recurrent neural network model," in *9th International Conference on Simulation and Adaptive Behavior*, vol. 4095, Rome, Italy, Sept. 25–29 2006, pp. 185–196.
- [23] V. Ivancevic and M. Snoswell, "Fuzzy-stochastic functor machine for general humanoid-robot dynamics," *IEEE Transactions on Systems, Man, and Cybernetics*, vol. 31, no. 3, pp. 319–330, June 2001.
- [24] Z. Tang, M. J. Er, and G. S. Ng, "Humanoid robotics modelling by dynamic fuzzy neural network," in *Proceedings of International Joint Conference on Neural Networks*, Orlando, Florida, USA, Aug. 12–17 2007, pp. 2653–2657.
- [25] T. Yamamoto and Y. Kuniyoshi, "Stability and controllability in a rising motion: a global dynamics approach," in *Proceedings of the 2002 IEEE/RSJ International Conference on Intelligent Robots and Systems*, EPFL, Lausanne, Switzerland, Sept. 30–Oct. 5 2002, pp. 2467–2472.
- [26] J. Park, Y. Youm, and W.-K. Chung, "Control of ground interaction at zero-moment point for dynamic control of humanoid robots," in *Proceedings of the 2005 IEEE International Conference on Robotics and Automation*, Barcelona, Spain, April 18–22 2005, pp. 1724–1729.
- [27] A. Bedford and W. Fowler, *Dynamics: Engineering Mechanics*. Reading, Mass.: Addison-Wesley, 1995.
- [28] K. S. Fu, R. C. Gonzales, and C. S. G. Lee, *Robotics: Control, Sensing, Vision, and Intelligence*. U.S.A.: McGraw-Hill, Inc., 1987.
- [29] O. Khatib, "A unified approach for motion and force control of robot manipulators: The operational space formulation," *International Journal of Robotics Research*, vol. RA-3, no. 1, pp. 43–53, 1987.
- [30] K. Ogata, *Modern Control Engineering*, 4th ed. Printice-Hall, Inc., 200.
- [31] L. Sentis and O. Khatib, "Synthesis of whole-body behaviors through hierarchical control of behavioral primitives," *International Journal of Humanoid Robotics*, vol. 2, no. 4, pp. 505 – 518, 2005.